Eur. Phys. J. D **14**, 147–155 (2001)

THE EUROPEAN PHYSICAL JOURNAL D

EDP Sciences

General theory of population transfer by adiabatic rapid passage with intense, chirped laser pulses

V.S. Malinovsky and J.L. Krause[a]

University of Florida, Quantum Theory Project, P.O. Box 118435, Gainesville, FL 32611–8435, USA

Received 6 September 2000 and Received in final form 25 September 2000

Abstract. We present a general theory of adiabatic rapid passage (ARP) with intense, linearly chirped laser pulses. For pulses with a Gaussian profile and a fixed bandwidth, we derive a rigorous formula for the maximum temporal chirp rate that can be sustained by the pulse. A modified Landau-Zener formula displays clearly the relationships among the pulse parameters. This formula is used to derive the optimal conditions for efficient, robust population transfer. As illustrations of the theory, we present results for two- and four-level systems, and selective vibronic excitation in the I_2 molecule. We demonstrate that population transfer with chirped pulses is more robust and more selective than population transfer with transform-limited pulses.

PACS. 33.80.-b Photon interactions with molecules – 42.50.-p Quantum optics

1 Introduction

The problem of population transfer in a two- (or n-) level system is a venerable one, dating back to the early days of quantum mechanics [1–4]. Renewed interest in this problem is a result of recent efforts to use lasers to control the course of chemical reactions [5–11]. Many proposed control schemes rely on the ability to start with a pure initial state, or an ensemble of identical initial states. For two-level systems, the method to create such states is well-known from the theory of magnetic resonance [12]. A narrow-band source of radiation is tuned to the resonance frequency. When the integrated area of the pulse is equal to π, complete population transfer occurs from the initial state to the final state.

The π-pulses method, while effective in certain cases, is not in general a robust method for population transfer. In particular, the results are highly sensitive to variations in the pulse area, and to inhomogeneities in the sample [13]. In addition, for an n-level system in which many initial states and final states lie within the bandwidth of the excitation source, it is virtually impossible for a single pulse to satisfy the π condition for all transitions simultaneously.

A much more robust method for population inversion is adiabatic rapid passage (ARP) [14–16]. In this scheme, the radiation is tuned above (or below) the resonance frequency, and the radiation (or the level itself) is swept through resonance. If the process is performed adiabatically, or

$$\sqrt{\Omega^2(t) + \Delta\omega^2(t)} \gg |\mathrm{d}/\mathrm{d}t\ \theta(t)|, \tag{1}$$

the desired final state can be populated with 100% efficiency [15]. In equation (1), $\Omega(t)$ is the Rabi frequency, $\Omega(t) = \mu E(t)$, where μ is the dipole moment and $E(t)$ is the laser field. The frequency detuning, $\Delta\omega(t)$, is defined as $\Delta\omega = \omega(t) - \omega_{12}(t)$, where $\omega_{12}(t)$ is the transition frequency, and $\omega(t)$ is the radiation frequency. The phase angle, $\theta(t)$, is given by $\theta(t) = \tan^{-1}[\Delta\omega(t)/\Omega(t)]$. Assuming that the temporal profile of the laser field is a slow function of time during the population transfer, and that $\Omega^2(t) \gg \Delta\omega^2(t)$. we can write this equation in the following simple form,

$$\Omega_0^2 \gg |\mathrm{d}/\mathrm{d}t\ \Delta\omega(t)|, \tag{2}$$

where Ω_0 is the peak Rabi frequency.

The first applications of ARP were performed in magnetic resonance [12,17]. In the optical regime, the initial experiments used a fixed laser frequency and a DC field to sweep the transition through resonance [18,19]. In another approach, a molecular beam was passed through a laser focus, and the curvature of the focus was used to provide the frequency sweep. More recent methods for population transfer *via* ARP include STIRAP (stimulated Raman adiabatic passage) [20], and its variants such as APLIP (adiabatic passage on laser induced potentials) [21,22], and time-gating [14,23]. In these methods, a pair of laser pulses is used to adiabatically couple an initial state and a final state through a third (generally non-populated) state. The timing between the pulses and the time-varying intensity profiles are used to achieve selectivity.

With the advent of short, intense pulses, and the development of laser pulse shaping technology, a new, and potentially more general method for selective population

[a] e-mail: krause@qtp.ufl.edu

transfer has emerged. Rather than relying on precise modifications to the potentials, it is now possible to apply the required frequency modulation directly to the excitation pulse [24–26]. This idea has been suggested as a way of performing ladder-climbing (sequential vibrational excitation) in small molecules [27–38]. One promising implementation is RCAP (Raman chirped adiabatic passage), in which two chirped pulses are used in an off-resonance Raman configuration [39,40]. Recently, use of a molecular "π pulse" using intense, positively chirped pulses, has been suggested as a general method for population transfer in molecules [41,42]. This method is a specific example of ARP by chirped pulses with large frequency bandwidths. Experimental verification of ARP has now been realized [15,16,43–45].

In this paper, we present a detailed analysis of the parameters governing the successful implementation of ARP. We derive a modified Landau-Zener formula that allows the important pulse parameters to be identified, and bounds to be placed on their values. Finally, we discuss a number of issues regarding experimental implementation of ARP that have sometimes been overlooked in the literature. As computational examples we consider generic two-level and four-level systems, and selective vibronic population transfer in iodine.

2 Basic properties of chirped laser pulses

In this section we review the basic properties of chirped laser pulses, and derive some relations among these parameters that will be useful in the following discussion. Many of the results in this section are well-known, or can be derived easily. We present them here for completeness, and for reference in the following discussion.

For simplicity we consider a Gaussian functional form for the electric field. We note that other forms, such as hyperbolic secant are possible, and may have advantages in certain applications [33]. The Gaussian field can be written

$$E(t) = E_0 \exp\left[-\frac{t^2}{2\tau^2} - \mathrm{i}\omega_0 t - \mathrm{i}\alpha\frac{t^2}{2}\right], \qquad (3)$$

where E_0 is the peak amplitude, $\tau\sqrt{\ln 16}$ is the pulse duration (full width at half-maximum, FWHM), ω_0 is the center frequency, and α is the linear temporal chirp. The Fourier transform of equation (3) can be performed analytically to give

$$E(\omega) = E_0' \exp\left[-\frac{(\omega-\omega_0)^2}{2\Gamma^2} + \mathrm{i}\alpha'\frac{(\omega-\omega_0)^2}{2}\right], \qquad (4)$$

where E_0' is the peak amplitude, $\Gamma\sqrt{\ln 16}$ is the frequency bandwidth (FWHM), and α' is the linear spectral chirp.

For simplicity in the following discussion, we will suppress the numerical factor $\sqrt{\ln 16}$ and refer to τ as the pulse duration and Γ as the bandwidth. We will also assume that the chirp is applied to the pulse using conventional linear optics (*e.g.*, *via* a grating or prism pair).

For transform-limited pulses (*i.e.*, pulses with zero chirp), $\Gamma = 1/\tau_0$, where τ_0 is the transform-limited pulse duration. However, for chirped pulses, the pulse duration and bandwidth depend on the chirp *via* the following relations,

$$\tau^2 = \frac{1}{\Gamma^2}\left(1+\alpha'^2\Gamma^4\right), \qquad (5)$$

and

$$\Gamma^2 = \frac{1}{\tau^2}\left(1+\alpha^2\tau^4\right). \qquad (6)$$

The linear temporal chirp and the linear spectral chirps are related by the following equations,

$$\alpha = \alpha'\frac{\Gamma^4}{(1+\alpha'^2\Gamma^4)}, \qquad (7)$$

and

$$\alpha' = \alpha\frac{\tau^4}{(1+\alpha^2\tau^4)}\,. \qquad (8)$$

As these formulas show, chirping a pulse increases its duration. To conserve the pulse energy, $P_0 = E_0^2\tau$, for a pulse with a fixed bandwidth, the peak intensity of the chirped pulse must be reduced as the duration increases. This is the principle behind the commonly-used chirped pulse amplifier [46], for example. The dependence of the intensity on the chirp is given by

$$I = I_0\frac{1}{\sqrt{1+\alpha'^2\Gamma^4}}, \qquad (9)$$

where I_0 is the peak intensity of the transform-limited pulse. In terms of the Rabi frequency, this equation can be rewritten as

$$\Omega_0 = \overline{\Omega}_0\frac{1}{\sqrt[4]{1+\alpha'^2\Gamma^4}}, \qquad (10)$$

in which $\overline{\Omega}_0$ is the peak Rabi frequency of the transform-limited pulse.

As can be seen in the above relations, the quantities α, α', Γ, τ and I are not independent, and are, in fact, related in a fairly complex fashion. The relationships among some of these quantities are shown in Figure 1. Note, in this figure, that α and α' have been scaled by τ_0^2. This gives the figure a universal form that is valid for all pulse durations and chirps. Note also that the range of α' is from $-\infty$ to $+\infty$, while α has a finite maximum and minimum value. The maximum temporal chirp can be determined from equation (7) to give

$$|\alpha_{\max}| = \frac{\Gamma}{2\tau_0} = \frac{1}{2\tau_0^2}\,. \qquad (11)$$

When $\alpha = \alpha_{\max}$, the value of the linear spectral chirp is

$$\alpha' = \pm\tau_0^2, \qquad (12)$$

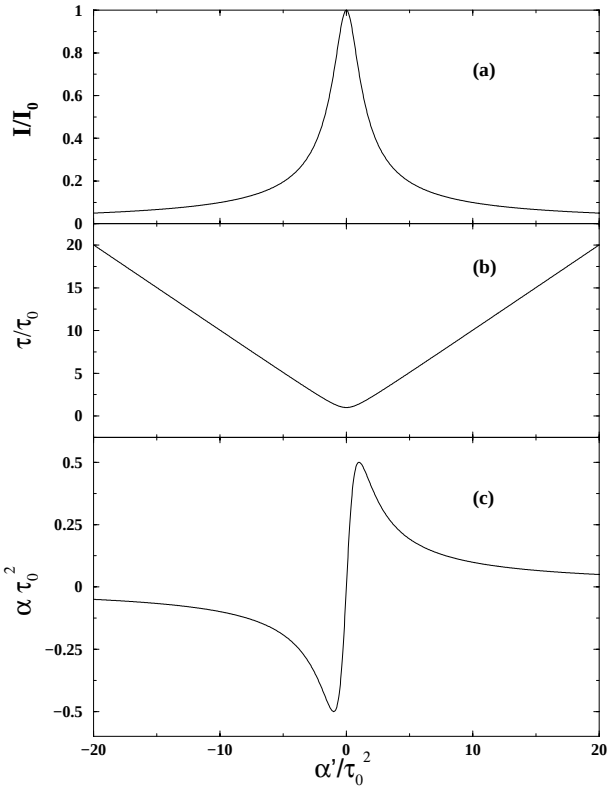

Fig. 1. Relationships among the parameters of linearly chirped Gaussian laser pulses for a pulse with a fixed frequency bandwidth. Panel (a) shows the dependence of the scaled intensity *versus* the scaled linear spectral chirp, panel (b) shows the scaled pulse duration versus the scaled linear spectral chirp, and panel (c) shows the scaled linear temporal chirp *versus* the scaled linear spectral chirp.

and the pulse duration is

$$\tau(\alpha_{\max}) = \sqrt{2}\tau_0. \tag{13}$$

Equation (11) expresses the physically reasonable (and exact mathematical) result that a laser pulse with a fixed bandwidth can sustain only a chirp large enough such that the bandwidth is chirped to zero over the duration of the pulse. This point must be considered when designing experiments for a laser system with a fixed bandwidth.

3 Modified Landau-Zener formula for ARP in two-level systems with chirped pulses

As an application of the results derived in the previous section, let us consider the case of population transfer in a two-level system. The optimal transfer occurs by sweeping the frequency through resonance at the center time of the pulse. This implies that $\Delta\omega = \alpha t$, where α is the linear temporal chirp. The Schrödinger equation for this system in the rotating wave approximation (RWA) is

$$\mathrm{i}\frac{\partial}{\partial t}\begin{pmatrix}\psi_1(t)\\ \psi_2(t)\end{pmatrix} = -\begin{pmatrix}0 & \Omega(t)/2\\ \Omega(t)/2 & \alpha t\end{pmatrix}\begin{pmatrix}\psi_1(t)\\ \psi_2(t)\end{pmatrix} \tag{14}$$

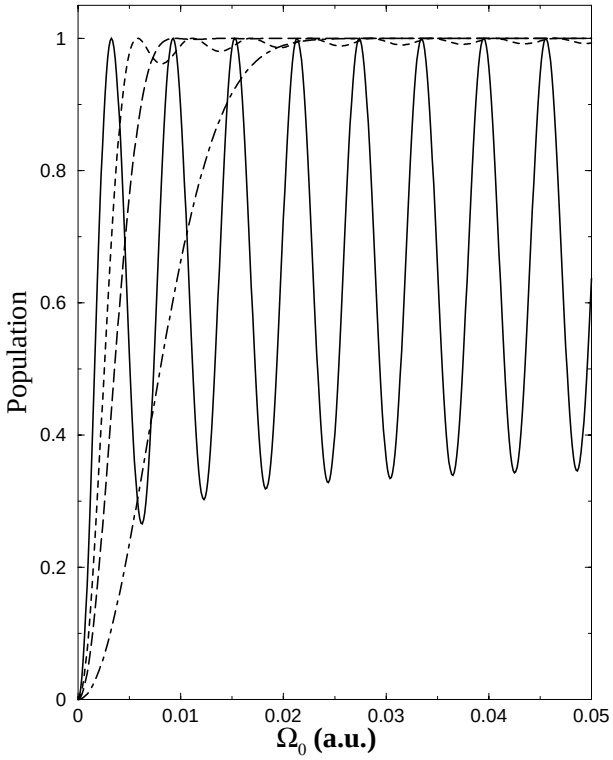

Fig. 2. Population transfer by adiabatic passage in two-level system. The duration of the pulse is $\tau_0 = 10$ fs. For the solid line, $\alpha = 0.5 \times 10^{-2}$ fs^{-2}, for the dashed line, $\alpha = 2.5 \times 10^{-2}$ fs^{-2}, for the long-dashed line, $\alpha = 5 \times 10^{-2}$ fs^{-2}, and for the dot-dashed line, $\alpha = 25 \times 10^{-2}$ fs^{-2}.

where $\Omega(t) = \mu_{12}E(t)/\hbar$ is the time-dependent Rabi frequency, μ_{12} is the dipole moment, and $E(t)$ is the pulse envelope.

As an example of the well-known dynamics of population transfer in a two-level system, Figure 2 shows the population transferred from the lower state to the upper state as a function of the peak Rabi frequency for several different values of the temporal chirp, α. The pulse duration, τ, in this figure is set to 10 fs. As can be seen in the figure, when $\alpha = 0.5\times10^{-2}$ fs^{-2}, 100% population transfer is achieved, but the results are not robust to small changes in the Rabi frequency. However, when $\alpha = 5.0\times10^{-2}$ fs^{-2} or larger, the results are quite robust.

Figure 2 can be interpreted in two different ways. First, with a transform-limited pulse the transition can be swept through resonance with an external DC field. In this case, the figure shows that a sweep rate of 5.0×10^{-2} fs^{-2}, or 266 cm^{-1}/fs, is required for robust population transfer. A second way of interpreting the figure is to assume that the transition frequency is fixed and the frequency sweep is achieved with a chirped laser pulse. Here, though, we must be careful about how the pulse parameters are specified. As shown in equation (6) a pulse duration of $\tau = 10$ fs and a chirp of $\alpha = 5.0 \times 10^{-2}$ fs^{-2} requires a bandwidth corresponding to a transform-limited pulse with a duration of $\tau_0 = 2.0$ fs. For a chirp of $\alpha = 25 \times 10^{-2}$ fs^{-2}, the corresponding transform-limited pulse is $\tau_0 = 0.4$ fs.

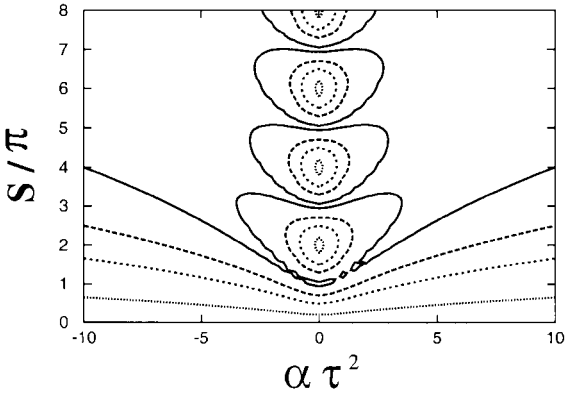

Fig. 3. Population transfer in a two-level system as a function of the pulse area S and scaled temporal linear chirp $\alpha\tau^2$. The center frequency of the laser is on-resonance with the transition. The isolines in the plot represent final yields of 0.99 (solid line), 0.80 (long-dashed line), 0.50 (dashed line), and 0.10 (dotted line).

This point has led to some confusion in the literature about the duration of a pulse required to achieve a desired outcome. For example, $\alpha_{\max}$ for a *transform-limited* pulse of 10 fs is 0.5×10^{-2} fs^{-2}. However, as can be seen in Figure 2, increasing α to a value greater than $\alpha_{\max}$ leads to more robust population transfer. Physically, though, such values of α imply that the bandwidth of the pulse increases during the chirping process. This is impossible if the chirp is applied *via* linear optics.

To analyze the robustness of ARP for a fixed pulse duration, Figure 3 shows a plot of the excited state population after the pulse is over as a function of the pulse area, S, where

$$S = \int \Omega(t)\mathrm{d}t = \sqrt{2\pi}\Omega_0\tau, \tag{15}$$

and the scaled temporal chirp rate, $\alpha\tau^2$. Once again, these scaled variables allow a universal plot of all possible pulse parameters (for a linearly chirped, Gaussian pulse). The figure shows pronounced areas of 100% population transfer near the π-pulse solutions, when $S = (2n+1)\pi$ and $\alpha = 0$. Roughly, as can be seen in the figure, robust areas of ARP are restricted by the conditions

$$|\alpha|\tau^2 \gg 1, \tag{16}$$

and

$$|\alpha|\tau^2 \ll \Omega_0^2\tau^2. \tag{17}$$

The latter relation is identical to the the adiabatic condition in equation (2). When this condition is obeyed, the Landau-Zener formula [2,3],

$$P_2 \approx 1 - \exp\left\{-\pi\frac{\Omega_0^2}{2\alpha}\right\}, \tag{18}$$

can be used to calculate the population transfer to the excited state. Note that the additional condition that the pulse duration, τ, must be much larger than the transition time, Ω_0/α [47,48],

$$\frac{\Omega_0}{\alpha} \ll \tau, \tag{19}$$

is not operational here. In general, when the adiabatic condition, equation (17), is satisfied, and the chirp is chosen according to equation (16), the parameters lie in the robust area of ARP, in which the Landau-Zener approximation is valid and accurate.

Figure 3 illustrates concisely the parameter ranges necessary for robust population transfer *via* ARP. However, for experimental implementation of ARP this representation is not the most convenient, because each point in Figure 3 corresponds to a laser pulse with a different frequency bandwidth. If, for example, τ is set to 10 fs, as α changes from 0 to 40×10^{-2} fs^{-2}, the bandwidth increases by nearly a factor of 40. Since most lasers operate at a fixed (or nearly fixed) bandwidth, a more meaningful representation is one in which the bandwidth is fixed. With a fixed bandwidth, the two independent parameters are the spectral chirp and the intensity (or peak Rabi frequency). All remaining parameters are determined by the relations in equations (5–10).

In the fixed bandwidth representation, the Landau-Zener formula can be written in terms of $\overline{\Omega}_0$, the peak Rabi frequency of the transform-limited pulse, and α', the linear spectral chirp. Using equations (7, 10, 18), we obtain

$$\begin{aligned} P_2 &\approx 1 - \exp\left\{-\pi\frac{\Omega_0^2}{2\alpha}\right\} \\ &= 1 - \exp\left\{-\frac{\pi\overline{\Omega}_0^2\tau_0^2}{2}\ \frac{\sqrt{1+\alpha'^2/\tau_0^4}}{\alpha'/\tau_0^2}\right\}. \end{aligned} \tag{20}$$

In this form of the Landau-Zener formula it is apparent that in the limit of

$$\alpha'/\tau_0^2 \gg 1, \tag{21}$$

we have the following limits for the pulse duration,

$$\tau \approx \frac{\alpha'}{\tau_0}, \tag{22}$$

and the chirp,

$$\alpha \approx \frac{1}{\alpha'}\cdot \tag{23}$$

In these limits, the Rabi frequency is

$$\Omega_0 \approx \overline{\Omega}_0\frac{\tau_0}{\sqrt{\alpha'}}, \tag{24}$$

and the Landau-Zener formula reduces to

$$P_2 \approx 1 - \exp\left\{-\frac{\pi}{2}\overline{\Omega}_0^2\tau_0^2\right\}. \tag{25}$$

It is clear from equation (25) that as τ_0 increases, P_2, the population on the excited state approaches its maximum

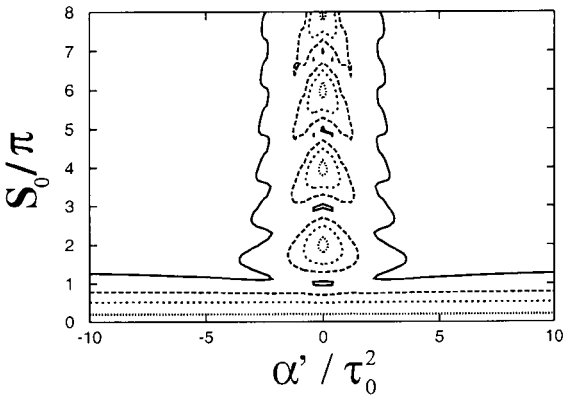

Fig. 4. Population transfer in a two-level system as a function of the transform-limited pulse area S_0 and scaled spectral linear chirp α'/τ_0^2. The center frequency of the laser is on-resonance with the transition. The isolines in the plot represent final yields of 0.99 (solid line), 0.80 (long-dashed line), 0.50 (dashed line), and 0.10 (dotted line).

value. Note, in this equation, that the population transfer is governed by the parameter

$$\epsilon = \overline{\Omega}_0^2 \tau_0^2, \tag{26}$$

which, in contrast to the conventional Landau-Zener formula (Eq. (18)), does not depend on the chirp rate. Since the condition of equation (21) is achieved readily with short femtosecond pulses, this analysis shows that the chirp is not the dominant factor in controlling population transfer over a large range of pulse widths and intensities. This observation may aid in the design of future experiments.

To investigate the robustness of population transfer *via* ARP with a fixed frequency bandwidth, Figure 4 shows a universal plot similar to Figure 3. In this case, however, the bandwidth is fixed, and the relevant variables are the scaled pulse area and the scaled linear *spectral* chirp. Once again, the π-pulse solutions are visible, and the robust areas are restricted by the adiabatic condition to

$$\overline{\Omega}_0^2 \, \tau_0^2 \gg 1, \tag{27}$$

and the limit described by equation (21).

Although Figures 3 and 4 are similar topologically, the difference between them is that all points in Figure 4 can be attained by a laser system with a single, fixed bandwidth. In Figure 3, however, each point requires a source with a different bandwidth. As the figures show, large areas of robust ARP can be achieved with chirped pulses, while the π-pulse solutions, as expected, have small areas of stability.

As a final note, we would like to point out that while ARP with a chirped laser pulse, and ARP *via* a sweep of the transition frequency can both produce robust population transfer, the methods differ both in the complexity of their implementation and in the physical limits on the pulse parameters. In the case of sweeping the transition frequency, the chirp can be varied independently of the intensity and pulse duration, while in the case of chirped-pulse ARP, the pulse parameters are coupled, and cannot be varied independently.

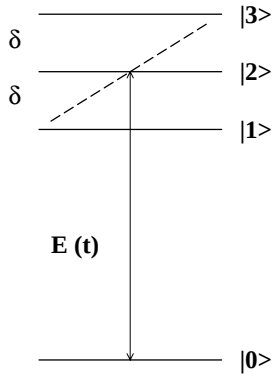

Fig. 5. Schematic for population transfer in a four-level system.

4 ARP in multi-level systems with chirped pulses

To generalize the results for the two-level system in the previous section, let us consider a system consisting of a single initial state and a manifold of final states, as in Figure 5. These states might be, for example, vibrational or rotational states in a molecule, or electronic states in an atom. The objective is to use a chirped, ultrafast laser pulse to selectively invert the population from the initial state to a selected final state. One scheme to do this has been demonstrated previously, both theoretically and experimentally by Melinger *et al.* [15,16]. By using a pulse with a bandwidth larger than the spacing between the levels, they showed that selective population transfer can be attained. With their method, however, it can be shown that only the uppermost or lowermost state in the excited manifold can be populated selectively [15,16,49].

Here we propose a more general scheme that has no restriction on the final state chosen, provided that the Franck-Condon factor between the initial state and the final state is not vanishingly small. In this method, the optimal laser pulse must have a bandwidth small enough to overlap significantly only the final state of interest. The frequency is tuned above (below) the desired final state, and the pulse is chirped negatively (positively) through resonance. If the pulse is intense enough to fulfill the adiabatic condition during the excitation process, the population is inverted selectively from the ground state to the excited state.

Results for the simple scheme in Figure 5 are presented in Figure 6. As can be seen in the figure, the area of robust population transfer has a similar topological structure to that in the two-level system. There are regions of efficient, though non-robust, population transfer by π pulses, and robust areas of transfer by ARP with positive and negative chirps. This figure suggests that by using an appropriate bandwidth and chirp, any final state in a manifold coupled to an initial state can be excited selectively. With intense pulses, a bandwidth smaller than the separation

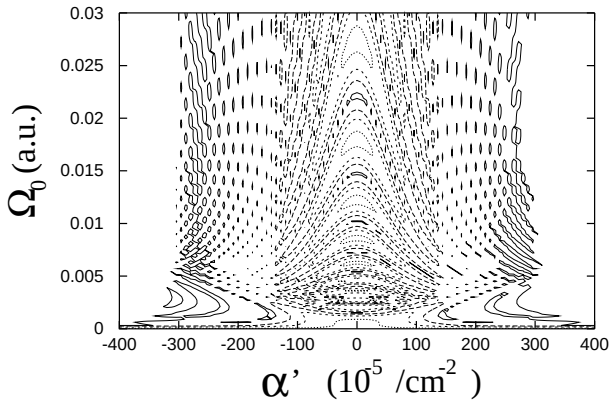

Fig. 6. Population transfer to state $|2\rangle$ in the four-level system depicted in Figure 5, as a function of the peak Rabi frequency Ω_0 and spectral linear chirp α'. The center frequency of the laser is on-resonance with the transition to state $|2\rangle$, the duration of the transform-limited pulse is $\tau_0 = 200$ fs, and the separation between states is $\delta = 400$ cm^{-1}. The isolines in the plot represent final yields of 0.99 (solid line), 0.80 (long-dashed line), 0.50 (dashed line), and 0.10 (dotted line).

between the levels, and the detuning set to zero at the time of maximum intensity, successful transfer is guaranteed, even when the peak Rabi frequency is larger than the separation between the states in the final-state manifold.

5 ARP in Iodine

As a realistic example of the model discussed above, we present results for selective population transfer from the X ground state to the B excited state in iodine (see Fig. 7). The initial state is the $v = 0$ level on the X state, and the final state is the $v' = 20$ level on the B state. For the numerical examples presented below, we choose a laser pulse with a bandwidth of 8.87 cm^{-1} (a transform-limited pulse length of 600 fs). The exact value of the bandwidth is not important, as long as it is less than ~ 90 cm^{-1}, the energy splitting on the B state near $v' = 20$.

Figure 8 shows the population transfer to the $v' = 20$ state for three different chirp rates. The population dynamics in this figure can be compared to the dynamics observed in the two-level system in Figures 2–4. For a transform-limited pulse, $\alpha = \alpha' = 0$, and, just as in the two-level system, 100% population transfer is possible, but the results are not robust to small changes in the Rabi frequency. With a chirp of $\alpha' = \tau_0^2$, or $\alpha = 7.4$ cm^{-1}/ps, which is the maximum value of α for this pulse duration, the population transfer is somewhat more robust. Interestingly, the population transfer becomes more robust as α' increases to $10\tau_0^2$, and α decreases to 2 cm^{-1}/ps. This corresponds to a point well out on the wings of the plot of α *versus* α' in Figure 1.

Although the results for iodine are similar to those in a two-level system, iodine cannot, in fact, be reduced to a two-level system. Considerable dynamics in the vibrational manifold occurs, the details of which are strongly

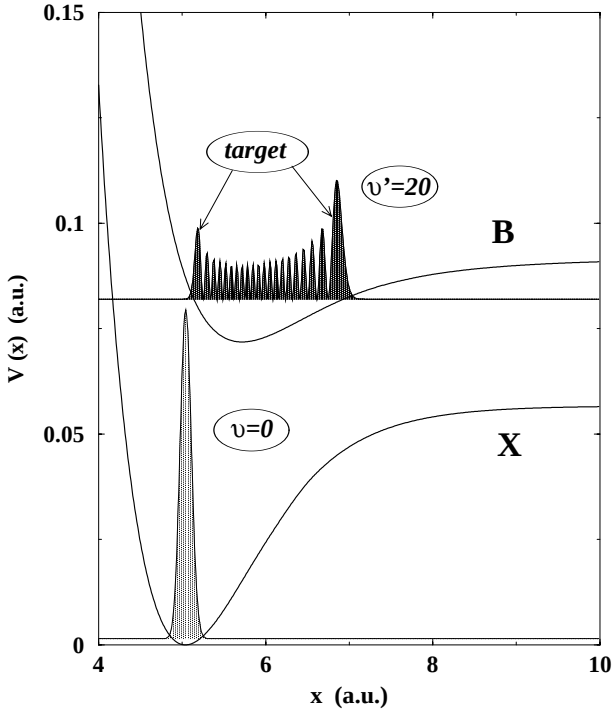

Fig. 7. Schematic for selective excitation of the 20th vibrational level of the B electronic state of I_2.

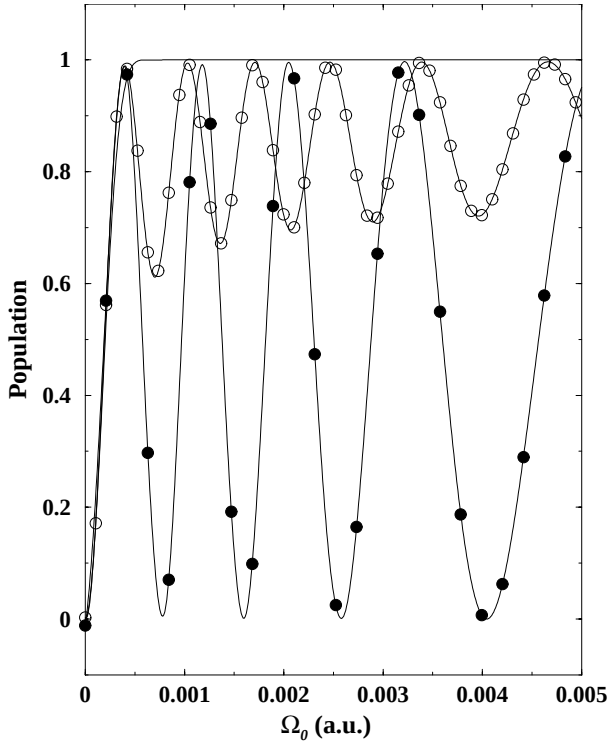

Fig. 8. Selective excitation of the 20th vibrational level of the B electronic state of I_2 as a function of the linear temporal chirp. The duration of the transform-limited pulse is $\tau_0 = 600$ fs. The three curves show the results for $\alpha = 0$ (filled circles), $\alpha = 7.4$ cm^{-1}/ps (open circles), and $\alpha = 2.0$ cm^{-1}/ps (solid line).

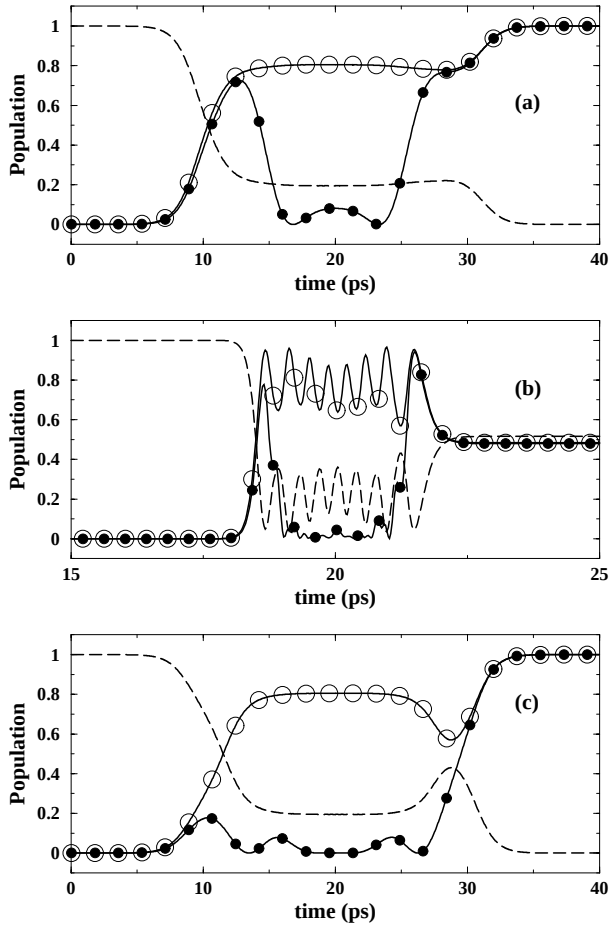

Fig. 9. Selective population transfer to the 20th vibrational level of the electronic B state of I_2. The duration and the Rabi frequency of the transform-limited pulse in each panel are $\tau_0 = 600$ fs, and $\Omega_0 = 0.03$ a.u. In panel (a), the temporal chirp rate is $\alpha = -2$ cm^{-1}/ps, in panel (b) $\alpha = 0$, and in panel (c), $\alpha = 2$ cm^{-1}/ps. The solid line with filled circles shows the population of the 20th vibrational level on the B state, the solid line with open circles shows the total population on the B state, and the dashed line shows the total population on the ground state.

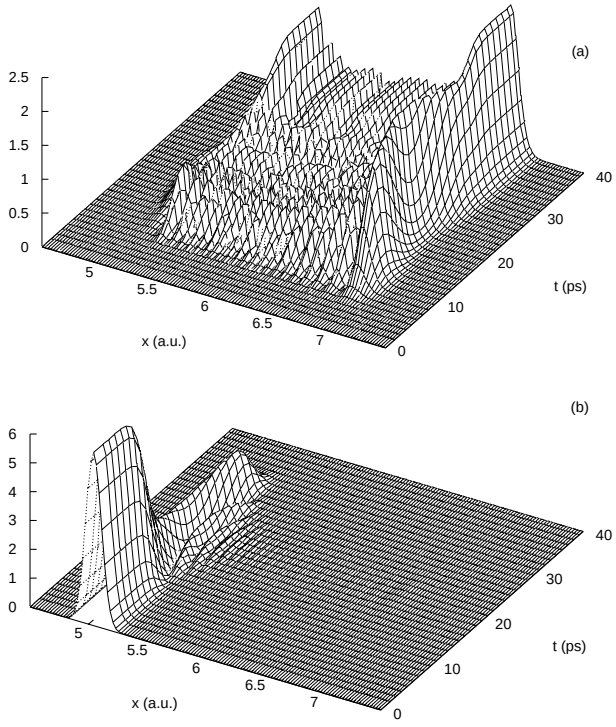

Fig. 10. Wave packet dynamics for the case of excitation by a pulse with a negative chirp. The initial state is $v = 0$ on the ground X state of I_2, and the target state is the $v' = 20$ on the B state. Panel (a) shows the wave packet amplitude, $|\psi(x,t)|^2$, on the excited state, and panel (b) shows the wave packet amplitude on the ground state. The pulse parameters are as in Figure 9a.

affected by the sign and magnitude of the chirp. Figure 9 illustrates population dynamics in the vibrational levels of ground and excited states for negative, zero and positive chirps. In this example, the chirped pulses achieve 100% selective population transfer, while the transform-limited pulse is only about 50% effective.

The vibrational dynamics during the excitation process are shown in Figures 10–12. Notice that in all cases wave packets are formed on both the ground and excited states, which implies that multiple vibrational states are involved in the process. Constructive and destructive interference of the population in these levels must be carefully controlled to meet the objective. It is interesting, in this regard, that both the negative chirp (Fig. 10) and the positive chirp (Fig. 12) are successful, yet their intermediate vibrational dynamics are quite different. We believe that the reason for this symmetry is that the adiabatic curve-crossing between the ground ($v = 0$) and target ($v' = 20$) vibrational levels occurs at the peak of the pulse. At this time, the dressed states responsible for population transfer with positive and negative chirps have the identical structure. They are, in fact, simply the time-reverse of each other. This symmetry can be destroyed by, for example, changing the detuning, which shifts the time at which the laser frequency sweeps through resonance. As a result, the dressed states are no longer symmetric about the crossing point, and the population transfer is no longer symmetric with respect to the sign of the chirp.

An additional difference between population transfer by pulses with negative and positive chirps in molecular systems is a result of the anharmonicity in the potentials. This causes variations in the Franck-Condon factors for transitions to vibrational states above and below the target state. Vibrational states above the target state are involved in the population dynamics for negative chirps, while states below the target state are important for the dynamics caused by positive chirps. In the iodine results presented here, the target state is not in the highly anharmonic region of the potential. As a result, the dynamics can compensate for the anharmonicity, and positive and negative chirps are equally effective.

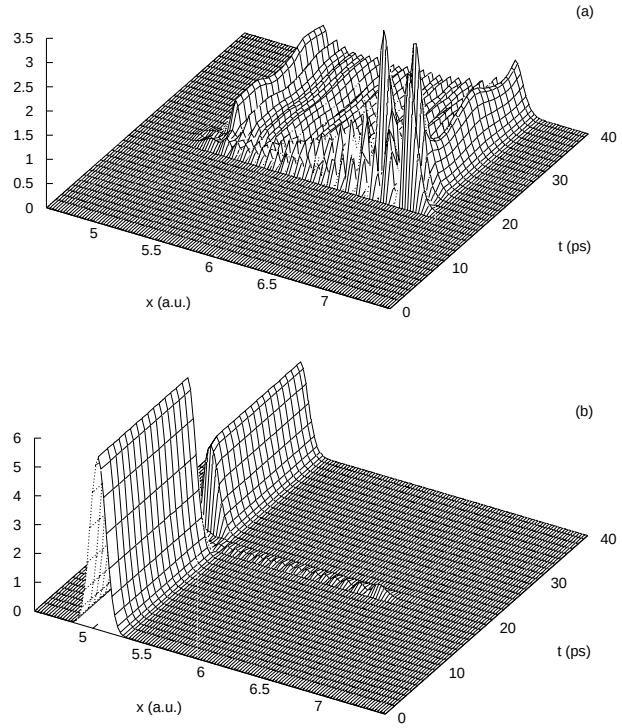

Fig. 11. Wave packet dynamics for the case of excitation by a transform-limited pulse. The initial state is $v = 0$ on the ground X state of I_2, and the target state is $v' = 20$ on the B state. Panel (a) shows the wave packet amplitude, $|\psi(x,t)|^2$, on the excited state, and panel (b) shows the wave packet amplitude on the ground state. The pulse parameters are as in Figure 9b.

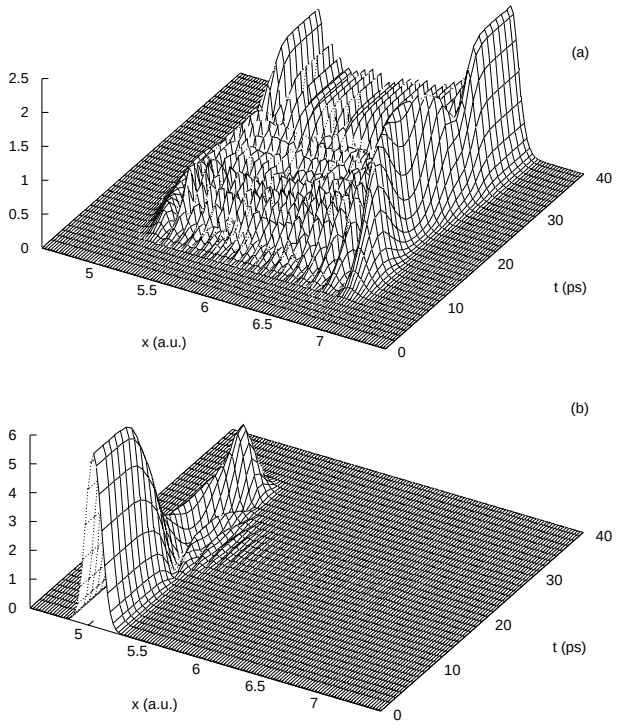

Fig. 12. Wave packet dynamics for the case of excitation by a pulse with a positive chirp. The initial state is $v = 0$ on the ground X state of I_2, and the target state is $v' = 20$ on the B state. Panel (a) shows the wave packet amplitude, $|\psi(x,t)|^2$, on the excited state, and panel (b) shows the wave packet amplitude on the ground state. The pulse parameters are as in Figure 9c.

6 Conclusions

In this paper we present a general theory of chirped ARP that attempts to unify similar phenomenology observed in diverse systems from population transfer in two-level systems to selective vibronic excitation in molecules. We derive relations to locate the areas of robust population transfer, and present a modified Landau-Zener formula to illustrate the relationships among the pulse parameters.

Our results show that in many systems the dominant effects governing efficient ARP are the Rabi frequency, the detuning, and the magnitude of the energy level spacing compared to the bandwidth of the laser pulse. The dynamics of population transfer in such cases is often symmetric with respect to the sign of the chirp. One example where this is not the case is selective vibronic excitation in an anharmonic potential. The I_2 results presented here show that when pulses with quite different chirps achieve efficient population transfer, the vibrational dynamics can differ significantly. We note that previous work has suggested that rotational states can adversely affect the selectivity of vibronic excitation [29,30]. Calculations are underway to investigate this effect.

Finally, we demonstrate that a class of experiments proposed theoretically may in fact be impossible, or more difficult than predicted due to fundamental limitations on the magnitude of the temporal chirp that can be applied to a pulse with a fixed bandwidth (using linear optics). This is not to say that such experiments cannot be performed using alternative schemes. However, the physical limitations involved in preparing chirped pulses must be considered when proposing schemes for experimental verification of theoretical predictions.

This work was partially supported by the National Science Foundation through grant CHE-9875080. JLK is a Cottrell Scholar of the Research Corporation.

References

1. I.I. Rabi, Phys. Rev. **51**, 652 (1937).
2. L.D. Landau, Phys. Z Sowj. **2**, 46 (1932).
3. C. Zener, Proc. R. Soc. Lond. A **137**, 696 (1932).
4. L. Allen, J.H. Eberly, *Optical Resonance and Two-Level Atoms* (John Wiley & Sons, Inc., New York, NY, 1975).
5. M. Shapiro, P. Brumer, Int. Rev. Phys. Chem. **13**, 187 (1994).

6. D.J. Tannor, S.A. Rice, Adv. Chem. Phys. **70**, 441 (1988).
7. D. Neuhauser, H. Rabitz, Acc. Chem. Res. **26**, 496 (1993).
8. W.S. Warren, H. Rabitz, M. Dahleh, Science **259**, 1581 (1993).
9. R.J. Gordon, S.A. Rice, Annu. Rev. Phys. Chem. **48**, 601 (1997).
10. J.L. Krause, R.M. Whitnell, K.R. Wilson, Y.J. Yan, in *Femtosecond Chemistry*, edited by J. Manz, L. Wöste (VCH, Weinheim, 1995), pp. 743–779.
11. S.A. Rice, M. Zhao, *Optical Control of Molecular Dynamics* (John Wiley & Sons, Inc., New York, NY, 2000).
12. A. Abragam, *Principles of Nuclear Magnetism* (Oxford Univ. Press, Oxford, England, 1961).
13. W.S. Warren, J.L. Bates, M.A. McCoy, M. Navratil, L. Mueller, J. Opt. Soc. Am. B **3**, 488 (1986).
14. *Molecules in Laser Fields*, edited by A. Bandrauk (Marcel Dekker, Inc., New York, NY, 1994).
15. J.S. Melinger, S.R. Gandhi, A. Hariharan, J.X. Tull, W.S. Warren, Phys. Rev. Lett. **68**, 2000 (1992).
16. J.S. Melinger, S.R. Gandhi, A. Hariharan, D. Goswami, W.S. Warren, J. Chem. Phys. **101**, 6439 (1994).
17. W.S. Warren, M.S. Silver, Adv. Mag. Res. **12**, 247 (1988).
18. M.M.T. Loy, Phys. Rev. Lett. **32**, 814 (1974).
19. M.M.T. Loy, Phys. Rev. Lett. **41**, 473 (1978).
20. K. Bergmann, H. Theuer, B.W. Shore, Rev. Mod. Phys. **70**, 1003 (1998).
21. B.M. Garraway, K.A. Suominen, Phys. Rev. Lett. **80**, 932 (1998).
22. I.R. Solá, J. Santamaría, V.S. Malinovsky, Phys. Rev. A **61**, 043413 (2000).
23. E.E. Aubanel, A.D. Bandrauk, J. Phys. Chem. **97**, 12620 (1993).
24. A.M. Weiner, J.P. Heritage, E.M. Kirschner, J. Opt. Soc. Am. B **5**, 1563 (1988).
25. C.W. Hillegas, J.X. Tull, D. Goswami, D. Strickland, W. Warren, Opt. Lett. **19**, 737 (1994).
26. M.M. Wefers, K.A. Nelson, Opt. Lett. **18**, 2032 (1993).
27. S. Chelkowski, A. Bandrauk, P.B. Corkum, Phys. Rev. Lett. **65**, 2355 (1990).
28. S. Chelkowski, A.D. Bandrauk, Chem. Phys. Lett. **186**, 264 (1991).
29. F. Legare, S. Chelkowski, A.D. Bandrauk, J. Raman, Spectrosc. **31**, 15 (2000).
30. J.C. Davis, W.S. Warren, J. Chem. Phys. **110**, 4229 (1999).
31. B. Just, J. Manz, I. Trisca, Chem. Phys. Lett. **193**, 423 (1992).
32. G.K. Paramonov, in *Femtosecond Chemistry*, edited by J. Manz, L. Wöste (VCH, Weinheim, 1995), pp. 671–711.
33. J.S. Melinger, McMorrow, C. Hillegas, W.S. Warren, Phys. Rev. A **51**, 3366 (1995).
34. M. Kaluza, J.T. Muckerman, J. Chem. Phys. **102**, 3897 (1995).
35. M. Kaluza, J.T. Muckerman, H. Rabitz, Chem. Phys. Lett. **225**, 335 (1994).
36. M. Kaluza, J.T. Muckerman, P. Gross, H. Rabitz, J. Chem. Phys. **100**, 4211 (1994).
37. M.N. Kobrak, S.A. Rice, Phys. Rev. A **57**, 2885 (1998).
38. S. Meyer, C. Meier, V. Engel, J. Chem. Phys. **108**, 7631 (1998).
39. S. Chelkowski, A.D. Bandrauk, J. Raman Spectrosc. **28**, 459 (1997).
40. S. Chelkowski, G. Gibson, Phys. Rev. A **52**, R3417 (1995).
41. J. Cao, C.J. Bardeen, K.R. Wilson, Phys. Rev. Lett. **80**, 1406 (1998).
42. J. Cao, C.J. Bardeen, K.R. Wilson, J. Chem. Phys. **113**, 1898 (2000).
43. D.J. Maas, D.I. Duncan, A.F.G. van der Meer, W.J. van der Zande, L.D. Noordam, Chem. Phys. Lett. **270**, 45 (1997).
44. D.J. Maas, D.I. Duncan, R.B. Vrijer, W.J. van der Zande, L.D. Noordam, Chem. Phys. Lett. **290**, 75 (1998).
45. D.J. Maas, M.J.J. Vrakking, L.D. Noordam, Phys. Rev. A **60**, 1351 (1999).
46. P. Maine, D. Strickland, P. Bado, M. Pessot, G. Mourou, IEEE J. Quantum Electron. **24**, 398 (1988).
47. N.V. Vitanov, B.M. Garraway, Phys. Rev. A **53**, 4288 (1996).
48. B.M. Garraway, N.V. Vitanov, Phys. Rev. A **55**, 4418 (1997).
49. V.S. Malinovsky, J.L. Krause, Phys. Rev. A (submitted, 2000).